INTERNATIONAL JOURNAL OF HYDROGEN ENERGY XXX (2012) 1–6

Available online at www.sciencedirect.com

SciVerse ScienceDirect

journal homepage: www.elsevier.com/locate/he

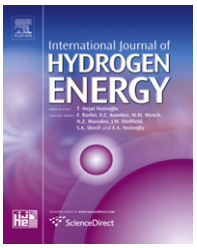

The cobalt content effect on the electrochemical behavior of nickel hydroxide electrodes

M.G. Ortiz [a,b,*], E.B. Castro [a], S.G. y Real [a]

[a] Instituto de Investigaciones Fisicoquímicas Teóricas y Aplicadas (INIFTA), Facultad de Ciencias Exactas, Universidad Nacional de La Plata, C.C.16, Suc. 4, 1900 La Plata, Argentina

[b] Facultad Regional La Plata, Universidad Tecnológica Nacional, Calle 60 y 124, La Plata, Argentina

ARTICLE INFO

Article history:
Received 26 August 2011
Received in revised form
16 December 2011
Accepted 31 January 2012
Available online xxx

Keywords:
Cathode in alkaline batteries
Nickel hydroxide
Metallic cobalt
Porous electrodes

ABSTRACT

In this paper, the study of nickel hydroxide porous electrodes containing different concentrations of cobalt as additive (2–10%), polytetrafluoroethylene (PTFE) as binder material and prepared by chemical impregnation on nickel sintered substrate, are presented. The characterization of the different electrodes is performed using optical techniques such as scanning electron microscopy (SEM), energy dispersive X-ray analysis (EDAX) and electrochemical techniques as cyclic voltammetry, charge-discharge curves and electrochemical impedance spectroscopy (EIS). The results indicate that the concentration of 5% metallic Co improves the electrochemical behavior of the active material.

1. Introduction

In the last years, much interest has been focused on the development of rechargeable alkaline batteries, trying to meet the demands resulting from technological innovations ranging from portable electronics to aeronautical and space applications or electric and hybrid-electric vehicles [1].

In alkaline batteries: Ni–Cd, Ni–Fe, Ni–Zn, Ni–MH and Ni–H, the positive electrode is nickel hydroxide. The electrochemical energy storage in this material is based on the reversible redox reaction, nickel hydroxide/oxhydroxide. The reversibility of this process is an important factor in the performance of nickel hydroxide as active material in the positive electrode. Another feature to consider is the poor electric conductivity of $Ni(OH)_2$ (p-type semiconductor), therefore, additives such as C, Ni, Co, Ca [2–5] are commonly used to improve the active material performance.

In the present work, a study, of the cobalt content effect, on the electrochemical behavior of nickel hydroxide electrodes is presented. The active material consisted of $Ni(OH)_2$ Aldrich and different concentrations of metallic Co (2%, 5% and 10%), 23% PTFE was added as binder material [2]. The mix was pasted onto the nickel foam substrate.

The electrodes were characterized using optical (SEM and EDAX) and electrochemical techniques such as cyclic voltammetry, charge-discharge curves and electrochemical impedance spectroscopy (EIS). The EIS experimental data are analyzed according to a physicochemical model, taking into account the porous nature of the electrode, and the faradaic process coupled to mass transport in the active material. Consequently, structural and kinetic parameters depending on the state of discharge (SOD) of the electrode can be identified, allowing to select the best electrode design.

* *Corresponding author*. Instituto de Investigaciones Fisicoquímicas Teóricas y Aplicadas (INIFTA), Facultad de Ciencias Exactas, Universidad Nacional de La Plata, C.C.16, Suc. 4, 1900 La Plata, Buenos Aires, Argentina. Tel.: +54 2214257430; fax: +54 2214254642.
E-mail address: mortiz@inifta.unlp.edu.ar (M.G. Ortiz).
0360-3199/$ – see front matter Copyright © 2012, Hydrogen Energy Publications, LLC. Published by Elsevier Ltd. All rights reserved.
doi:10.1016/j.ijhydene.2012.01.160

2. Experimental

2.1. Preparation of the working electrodes

The working electrodes used for the experiments were prepared on a nickel sintered substrate. The active material consisted of $Ni(OH)_2$ Aldrich containing 23% PTFE and different concentrations of metallic Co, electrode A: 2%, electrode B: 5% and electrode C: 10%. All were pressed with 200 kg/cm^2.

2.2. Characterization using optical techniques

The SEM images were obtained using a scanning electron microscope Philips SEM model 505 with an image digitizer System Soft Imaging ADDA II. The EDAX mapping tests were performed using an ESEM FEI Quanta 200 model microscope. This instrument has an energy dispersive X-ray analysis system, EDAX, Apollo 40 model.

2.3. Electrochemical characterization

A three-compartment electrochemical cell was employed for the electrochemical experiments. The electrolyte was a 7 M KOH solution at 30 °C. A nickel mesh of large specific area was used as counter-electrode and a Hg/HgO electrode, was used as reference electrode.

The charge-discharge curves at different current densities, the cyclic voltammetry with anodic and cathodic limits to potential default values (0.05 V and 0.7 V respectively) and at scanning rate of 50 mV s^{-1}, were performed using a kit Arbin BT2000 model potenciostat.

EIS measurements were carried out potentiostatically at the open circuit potential attained at each SOD, employing a frequency response analyzer Solartron 1250 coupled to a potentiostat EG&G model PAR 273. Measurements were carried out in the 3.15 mHz $\leq f \leq$ 65 KHz frequency range, with a sinusoidal signal perturbation of small amplitude (5 mV), to guarantee a constant state of discharge.

3. Results and discussion

3.1. Optical techniques

3.1.1. SEM

SEM technique was used to evaluate the surface morphology of the working electrodes. Fig. 1(a–c) exhibit the surface morphology, at a magnification of 500×, of the electrode A, B and C respectively.

The micrographs show that the electrodes A and C have a compact surface morphology, unlike the electrode B, whose surface morphology appears to be a more porous structure with better defined holes or pores.

3.1.2. EDAX

The EDAX mapping analysis carried out by EDAX technique was used to identify the distribution of cobalt in the active material. Fig. 2(b,d,f) shows the EDAX results for the electrodes A, B and C respectively. Fig. 2(a,c,e) shows the corresponding SEM images of the regions analyzed by EDAX, for each electrode, with a magnification of 500×.

Fig. 2 exhibits differences in the distribution of metallic cobalt in the active material depending on Co concentration. Results corresponding to electrodes A and B indicate a more uniform cobalt distribution compared to that exhibited by electrode C. For this electrode areas of higher concentration of cobalt were clearly seen.

3.2. Electrochemical techniques

3.2.1. Cyclic voltammetry

Fig. 3 shows the stabilized voltammograms corresponding to electrodes A, B and C, after 30 cycles at a scan rate of 50 mV s^{-1}. Voltammetric peaks associated with the redox reaction $Ni(OH)_2$/NiOOH are observed.

Voltammetric results indicate the better reversibility associated with the redox process, for electrode B, together with a significant decrease in the oxygen evolution reaction overpotential.

3.2.2. Discharge curves

Fig. 4 depicts discharge curves, at 1 mA, corresponding to electrodes A, B and C. The electrodes were previously loaded to their maximum capacity. It can be seen in Fig. 4 that electrode B exhibits the best capacity at 1 mA, in comparison to the values presented by electrodes A and C.

3.2.3. Electrochemical impedance spectroscopy

3.2.3.1. Theoretical model. The impedance response corresponding to nickel hydroxide electrodes was analyzed in terms of a physicochemical model which accounts for the charge/discharge process, taking place at the active material/electrolyte interface of the porous structure of the electrode. The working electrode is described as a porous flooded structure, conformed by spherical NiOOH particles. The faradaic process is related to the charge transfer reaction coupled to the diffusion transport of protons in the active material [6–8].

The impedance function of the porous structure, Z_p may be expressed as [7]:

$$Z_P(j\omega) = \frac{L}{A_{gt}k}\left(\frac{1}{\nu(j\omega)\tanh\nu(j\omega)}\right) \quad (1)$$

Being: $\nu(j\omega) = L(\frac{1}{k})^{1/2}Z_i^{-1/2}(j\omega)$

Where L is the thickness of the electrode, A_{gt} the geometric area, k the effective conductivity of the electrolyte and Z_i the interfacial impedance of the active material/electrolyte interface per unit volume (Ω cm^3). Z_i, is related to the parallel connection between the impedance of the double layer capacitance (Z_{dc}) and the faradaic impedance (Z_f).

$$Z_i^{-1} = Z_{dc}^{-1} + Z_F^{-1} \quad (2)$$

$$\text{Being}: \quad Z_{dc} = \frac{1}{j\omega C_{dc}a_e} \quad Z_F = \frac{Z_f}{a_a} \quad (3)$$

$j = \sqrt{-1}$, C_{dc} double layer capacitance per unit interfacial area ($C_{dc} \approx 5 \times 10^{-5}$ F cm^{-2}), a_e interfacial area per unit volume

Please cite this article in press as: Ortiz MG, et al., The cobalt content effect on the electrochemical behavior of nickel hydroxide electrodes, International Journal of Hydrogen Energy (2012), doi:10.1016/j.ijhydene.2012.01.160

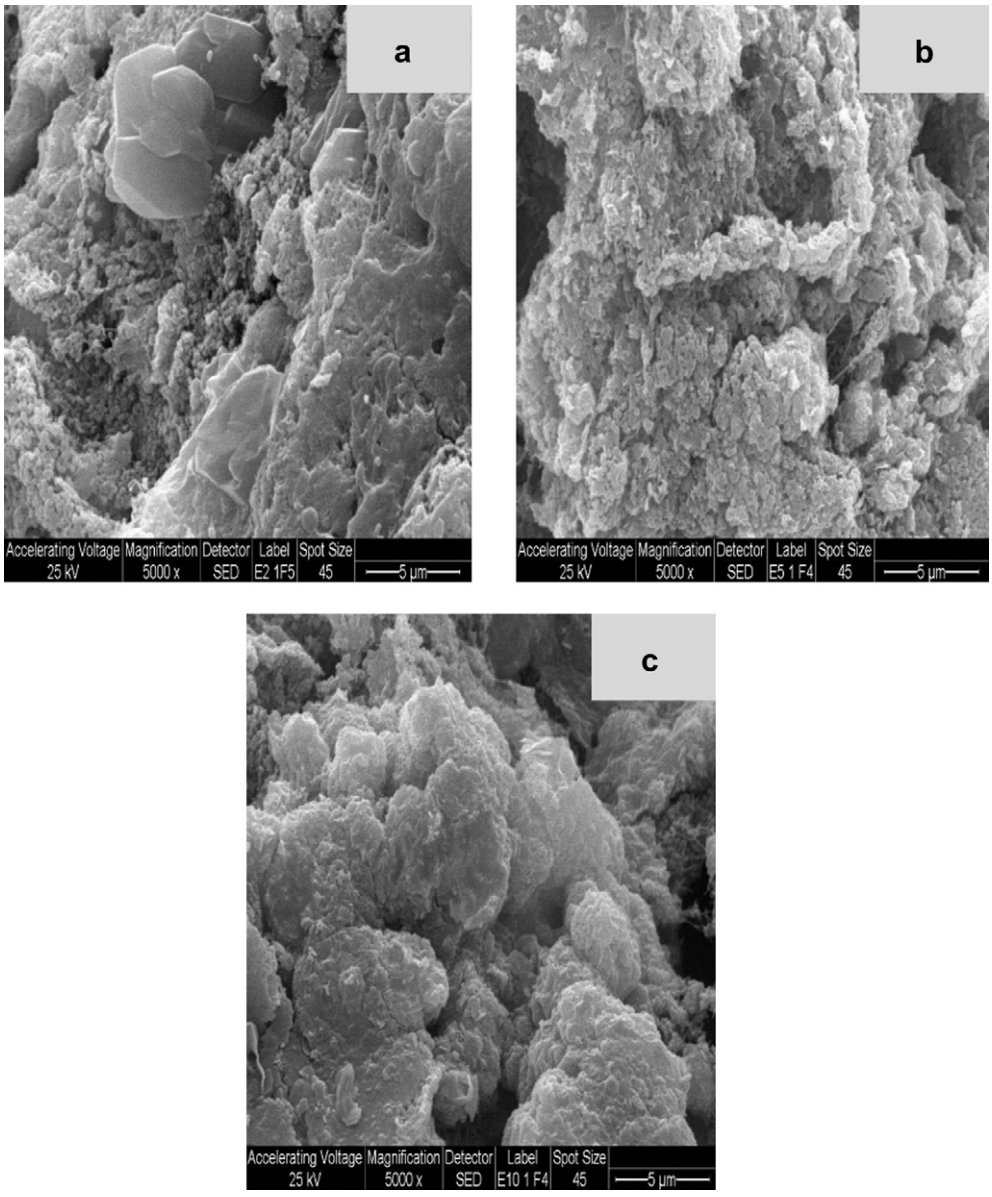

Fig. 1 – SEM micrographs, (a) electrode A, (b) electrode B y (c) electrode C.

(cm^{-1}) and $\omega = 2\pi f$ (f, frequency of the perturbing signal, in Hz). Z_f is the faradaic impedance per unit interfacial area ($\Omega\ cm^2$) and a_a is the active area per unit volume (cm^{-1}).

In the derivation of Z the active material was modeled as a solid solution of NiOOH, whose composition varies during the charge/discharge due to the insertion of protons [8]. Z_f, for this system has been derived in previous publications [9]:

$$Z_f(j\omega) = R_T - \frac{RTM(j\omega)}{F^2X(1-X)} \quad (4)$$

Being: $X = (1 - SOC)_{Ni}$, i^0_{Ni} the exchange current density of nickel electrode at the state of charge (SOC) for the EIS measurement, $M(j\omega)$ the mass transfer function associated with proton diffusion in spherical particles of active material, is derived, solving Fick's laws for spherical geometry with the adequate boundary condition [10,11].

Thus the total impedance of the electrode (Z_P) can be calculated from equations (1–4) [9,11]. The fitting procedure of experimental impedance data in terms of Z_p, allows the identification of structural and kinetic parameters of the studied system.

3.2.3.2. *Experimental results*. Fig. 5 shows EIS results as Nyquist plots, for different states of discharge. The experimental spectra are compared with the theoretical results obtained according to the above described physicochemical model. A good agreement between experimental and theoretical results is exhibited in Fig. 5.

For all studied systems, the impedance values were found to increase with increasing discharge state.

EIS results were fitted according to the described model and the kinetic and structural parameters governing

Please cite this article in press as: Ortiz MG, et al., The cobalt content effect on the electrochemical behavior of nickel hydroxide electrodes, International Journal of Hydrogen Energy (2012), doi:10.1016/j.ijhydene.2012.01.160

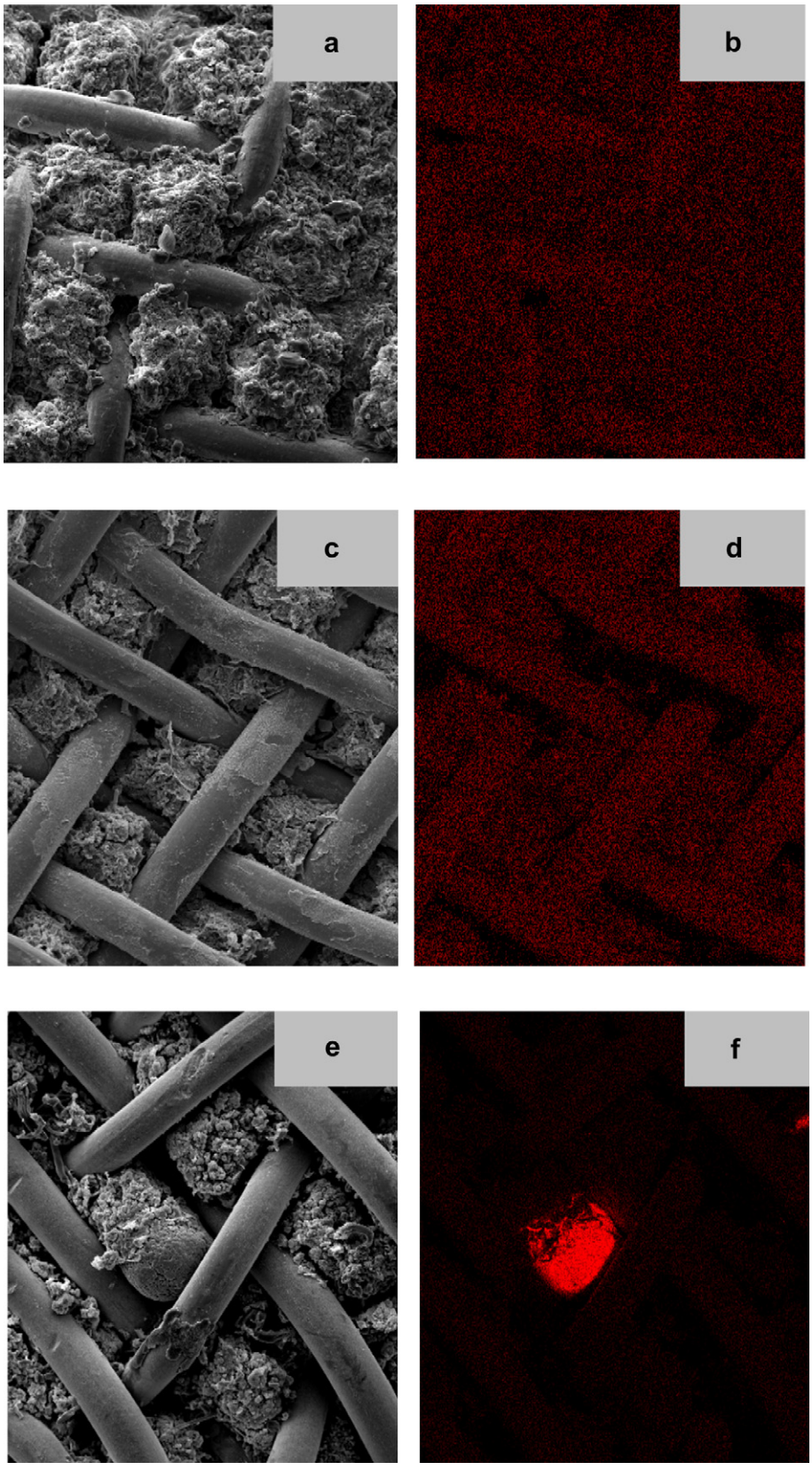

Fig. 2 – EDAX mapping analysis: electrode A (a) y (b), electrode B (c) y (d) y electrode C (e) y (f).

Please cite this article in press as: Ortiz MG, et al., The cobalt content effect on the electrochemical behavior of nickel hydroxide electrodes, International Journal of Hydrogen Energy (2012), doi:10.1016/j.ijhydene.2012.01.160

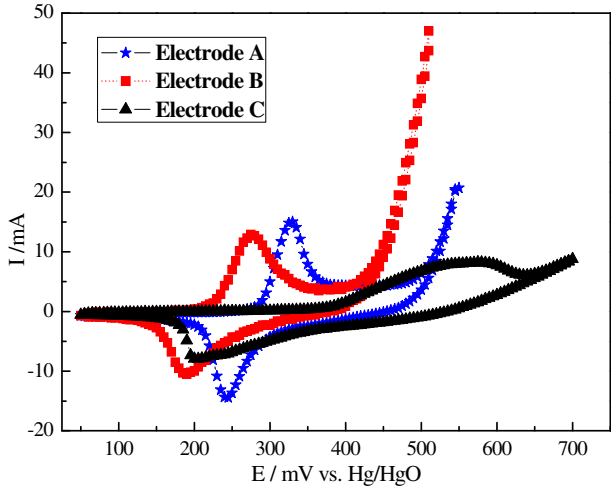

Fig. 3 – Cyclic voltammograms of electrodes A, B and C.

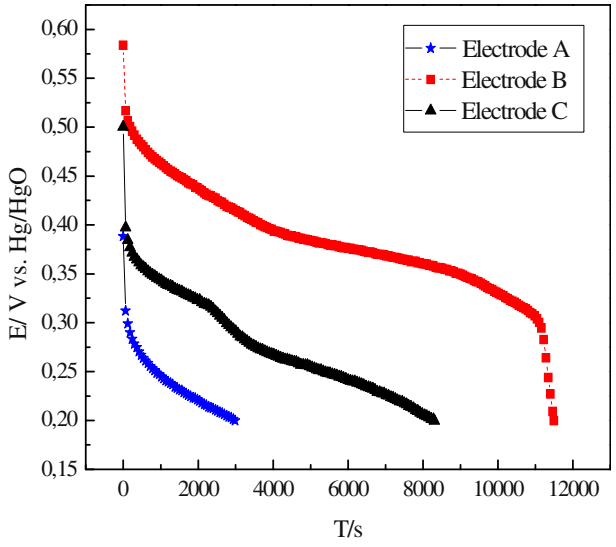

Fig. 4 – Discharge curves of electrodes A, B and C.

Table 1 – Parameters derived from experimental data fitting for the electrode A.

SOD	C_{dl} [F]	k [Ω^{-1} cm^{-1}]	a_e (cm^{-1})	D [cm^2 s^{-1}]	i_{oNi} [A cm^{-2}]
0.2	0.5	0.003	10×10^3	1.5×10^{-13}	4.0×10^{-5}
0.4	0.4	0.002	8.2×10^3	3.0×10^{-13}	5.0×10^{-5}

Table 2 – Parameters derived from experimental data fitting for the electrode B.

SOD	C_{dl} [F]	k [Ω^{-1} cm^{-1}]	a_e (cm^{-1})	D [cm^2 s^{-1}]	i_{oNi} [A cm^{-2}]
0.2	0.8	0.045	16.2×10^3	1.3×10^{-13}	1.0×10^{-4}
0.4	0.6	0.040	12.4×10^3	1.4×10^{-13}	1.4×10^{-4}

Table 3 – Parameters derived from experimental data fitting for the electrode C.

SOD	C_{dl} [F]	k [Ω^{-1} cm^{-1}]	a_e (cm^{-1})	D [cm^2 s^{-1}]	i_{oNi} [A cm^{-2}]
0.2	3.1	0.008	62.4×10^3	6.2×10^{-13}	8.0×10^{-6}
0.4	1.6	0.009	31.8×10^3	3.0×10^{-13}	9.0×10^{-6}

electrochemical behavior of the system were identified. The obtained parameter values are shown in Tables 1–3.

The electrical capacity associated with the charge of double layer (interfacial electrical capacity per unit volume, Cdl), for each electrode, decreases when the state of discharge increases. This parameter shows higher values for the electrode C, and consequently greater interfacial area per unit volume (a_e).

The values of k, a parameter which is proportional to the porosity of the electrode, are lower for electrodes A and C, therefore we can conclude that the porosity of electrode B is higher.

A nearly constant of exchange current density (i_{oNi}) values for different SOD were found. However, the exchange current density values are higher for the electrode B. This fact can be related to a better homogeneous distribution cobalt concentration ratio in the active material.

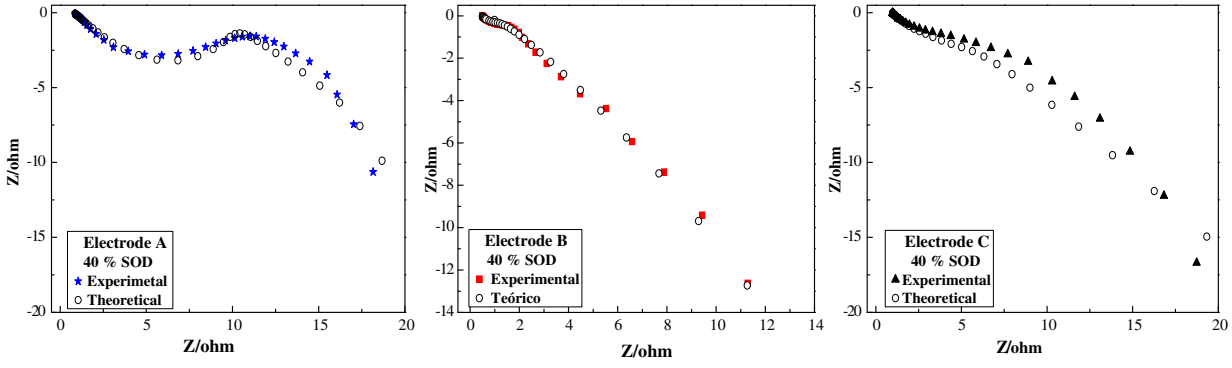

Fig. 5 – Nyquist plots for the electrode A, B and C.

Please cite this article in press as: Ortiz MG, et al., The cobalt content effect on the electrochemical behavior of nickel hydroxide electrodes, International Journal of Hydrogen Energy (2012), doi:10.1016/j.ijhydene.2012.01.160

4. Conclusions

The analysis of the results allows to conclude that the addition of 5% metallic Co as additive in electrodes of $Ni(OH)_2$ improves the distribution of cobalt in the active material and increases in one order the value of the exchange current density. These facts are in agreement with an increase the discharge capacity, better reversibility and a decrease in the overpotential associated to both oxidation–reduction process and the oxygen evolution reaction. Therefore, the 5% metallic Co concentration improves the operation performance of the electrodes.

Acknowledgments

The authors acknowledge the financial support given by the following Argentina organizations: Agencia Nacional de Promoción Científica y Tecnológica (ANPCyT), Consejo Nacional de Investigaciones Científicas y Técnicas (CONICET) and Universidad Tecnológica Nacional (UTN).

REFERENCES

[1] Casas-Cabanas M, Hernández JC, Gil V, Soria ML, Palacín MR. On the key importance of homogeneity in the electrochemical performance of industrial positive active materials in nickel batteries. J Power Sources 2004;134:298–307.

[2] Shao-an Cheng, Leng Wenhua, Jianqing Zhang, Chunan Cao. Electrochemical properties of the pasted nickel electrode using surface modified $Ni(OH)_2$ powder as active material. J Power Sources 2001;101:248–52.

[3] Wang Xianyou, Luo Hean, Yang Hongping, Sebastian PJ, Gamboa SA. Oxygen catalytic evolution reaction on nickel hydroxide electrode modified by electroless cobalt coating. Int J Hydrogen Energy 2004;29:967–72.

[4] Nathira Begum S, Muralidharan VS, Ahmed Basha C. The influences of some additives on electrochemical behaviour of nickel electrodes. Int J Hydrogen Energy 2009;34:1548–55.

[5] Zhu Wen-Hua, Ke Jia-Jun, Yu Hong-Mei, Zhang Deng-Jun. A study of the electrochemistry of nickel hydroxide electrodes with various additives. J Power Sources 1995;56:75–9.

[6] De Levie R. In: Delahay P, editor. Advances in electrochemistry and electrochemistry engineering, vol. 6. NY: Interscience; 1967. p. 329–61.

[7] Meyers JP, Doyle M, Darling RM, Newman J. The impedance response of a porous electrode composed of intercalation particles. J Electrochem Soc 2000;147:2930–40.

[8] Motupally S, Streinz CC, Weidner JW. Proton diffusion in nickel-hydroxide films – measurement of the diffusion-coefficient as a function of state of charge. J Electrochem Soc 1995;142:1401–8.

[9] Castro EB, Cuscueta DJ, Milocco RH, Ghilarducci AA, Salva HR. An EIS based study of a Ni–MH battery prototype. Modeling and identification analysis. Int J Hydrogen Energy 2010;35:5991–8.

[10] Jacobsen T, West K. Diffusion impedance in planar, cylindrical and spherical symmetry. Electrochim Acta 1995;40:255–62.

[11] Real SG, Ortiz MG, Castro EB, Visintin A, Becker D, Garaventta G. Dynamic monitoring of structural changes in nickel hydroxide electrodes during discharge in batteries. Electrochim Acta 2011;56(23):7946–54.

Please cite this article in press as: Ortiz MG, et al., The cobalt content effect on the electrochemical behavior of nickel hydroxide electrodes, International Journal of Hydrogen Energy (2012), doi:10.1016/j.ijhydene.2012.01.160